

Supplementary Information

Analytical model

Here, we present an analytical model based on that presented by Agrawal [1]. We consider an infinite population of haploid hermaphrodites with discrete non-overlapping generations. Individuals are characterized by the same two loci as in the simulation model. Because we are interested in maternal infection, we must keep track of an individual's ancestry at the **A**-locus. Therefore, we let $x_{i,j;k}$ denote the frequency of genotype (i, j) individuals that are born to a mother with antigen genotype k . The pair of indices (i, j) denotes the individual's genotypes at the **A**-locus and **M**-locus, respectively. For example, $x_{A,M;a}$ denotes the frequency of individuals of genotype (A, M) born to mothers of genotype a .

Each generation individuals first reproduce sexually. During reproduction, mutation occurs between alternative alleles at the antigen locus with probability m_j , where j denotes an individual's genotype at the modifier locus ($j = m$ or $j = M$). The frequency of eggs of genotype (i, j) produced by mothers of antigen type k is, therefore, given by

$$e_{i,j;k} = \sum_g (1 - m_j)d_{i,k} + m_j(1 - d_{i,k}) x_{k,j;g}, \quad (\text{S1})$$

where $d_{i,k}$ is an indicator function that equals 1 if $i = k$ and 0 if $i \neq k$. The sum over g

19 Note that we assume there is no paternal transmission, and so we do not track the an-
 20 cestry of the father. Summing over all sperm donors' antigen types (i.e. over all k), in
 21 addition to over all grandmother types, accomplishes this.

22 Sperm and eggs are assumed to unite randomly and in proportion to their frequencies.
 23 We let $f_{(m,n;o) (p,q)} = e_{m,n;o} s_{p,q}$ denote the frequency of unions between $(m, n; o)$ eggs and
 24 (p, q) sperm. These unions produce transient diploids that then undergo meiosis, with
 25 recombination occurring between loci at rate r . The genotype frequencies after meiosis
 26 are given by

$$x_{i,j;k}^{\theta} = \sum_{m,n,o,p,q} f_{(m,n;o) (p,q)} Y_{i,j;k,(m,n;o) (p,q)}, \quad (\text{S3})$$

27 where $Y_{i,j;k,(m,n;o) (p,q)}$ is the fraction of offspring of type $(i, j; k)$ resulting from meiosis
 28 with recombination of the transient diploid produced by the union of $(m, n; o)$ eggs and
 29 (p, q) sperm.

30 Selection follows reproduction. There are two primary components to selection in our
 31 model. First, we assume there is maternal infection, in the form of similarity selection,
 32 as described above. An individual that differs from its mother at the **A**-locus will have
 33 similarity fitness (denoted w_S) equal to 1, while an individual with the same genotype
 34 will have similarity fitness $w_S = 1 - g$. By imposing a penalty for sharing the same allele
 35 as one's mother at the **A**-locus, we are implicitly adopting an immunity model in which
 36 parasites target hosts on the basis of genotype, such as the matching alleles model used
 37 in the simulations.

38 Second, we assume that there is "genotypic selection" at the **A**-locus. This component
 39 of an individual's fitness represents selection imposed by the global parasite pool and is,
 40 therefore, independent of ancestry. We assign genotypic fitnesses (w_G) of 1 and $1 - a$ to
 41 the A and a alleles, respectively. When a is positive (respectively, negative), individuals
 42 with an A allele have a higher (respectively, lower) genotypic fitness. For convenience,

43 we assume that a is positive in what follows. Although fluctuations in genotypic selec-
 44 tion would be expected in a model of host-parasite coevolution under many parameter
 45 regimes, as observed in our simulations (Fig. 2) and in previous work [2], for sake of
 46 tractability, we do not allow such fluctuations to occur here. Our analytical model, there-
 47 fore, approximates the dynamics that would occur during periods when parasites that
 48 can infect individuals with the a -allele predominate.

49 The above two fitness components act multiplicatively to determine an individual's
 50 total fitness. An individual with genotype i at the **A**-locus, born to a mother with allele k
 51 at the **A**-locus, has fitness

$$w_{i;k} = w_S w_G = (1 - g)^{d_{i,k}} (1 - a)^{d_i}, \quad (\text{S4})$$

52 where $d_{i,k}$ equals 0 when $i \neq k$ and 1 when $i = k$, and d_i equals 0 when $i = A$ and 1 when
 53 $i = a$. The genotype frequencies after selection can then be computed as

$$x_{i;j;k}^{00} = \frac{x_{i;j;k}^0 w_{i;k}}{\bar{w}}, \quad (\text{S5})$$

where \bar{w}

58 QLE analysis

59 We performed a QLE (Quasi-Linkage Equilibrium) analysis to examine the rate at which
60 evolution occurs at the modifier locus [3]. Briefly, the QLE analysis assumes that selection
61 and mutation are weak relative to recombination and segregation and thus that allele fre-
62 quency changes at the **A** and **M** loci occur slower than changes in the various associations
63 among the loci (e.g., linkage disequilibrium). Using this separation of time scales allows
64 us to assume that the associations are always at their steady-state values, which greatly
65 simplifies analysis.

66 We assume that the modifier allele, M , has an effect of increasing the mutation rate by
67 Dm from the baseline value m_m encoded by the m allele (i.e., $m_M = m_m + Dm$). In order to
68 perform the QLE analysis, we assume that selection and mutation are weak relative to re-
69 combination. We begin by following Agrawal (2006) and assuming that a is on the order
70 of some small term, z , and that g is of even smaller order, z^2 . We further assume that the
71 mutation rate, m_m , and the effect of the modifier, Dm , are also of order z^2 . Due to these
assumptions, changes in allele frequency occur much more slowly than changes in asso-

where $D_{A,M}$

96 where V_M is the variance at the **M**-locus. Similarly computing DP_M to higher order and
97 substituting this steady-state value for $D_{A,M}$ yields

$$DP_M = \frac{2(1-r)}{r} a D m (1/2 - P_A) V_M z^3 + O(z^4). \quad (\text{S11})$$

98 From Eq. S11, we can see that the rate and direction of change in the modifier depends
99 only on the strength of genotypic selection (a), and that higher mutation rates are selected
100 against when the beneficial A -allele is at a frequency greater than $1/2$. We can also see
that lower rates of recombination, r

119 single generation is equal to

$$DP_A = V_A(a + g(1/2 - P_A))z + O(z^2) \quad (\text{S12})$$

120 and the change in frequency of the M -allele is

$$DP_M = D_{A,M}((1 - r)a + g(1/2 - P_A))z + O(z^2) \quad (\text{S13})$$

121 Repeating what we did in the first QLE analysis, we find that the recursions for the associ-
122 ation measures over one time step are the same as those in Eq. S9 and that the steady-state
123 solution for $D_{A,M}$ is the same as in Eq. (S10). Repeating the procedure described above,
we find the leading order change in the frequency of the M

135 *J. Theor. Biol.*, **140**, 499–518.

136 [3] Barton, N. H. & Turelli, M. 1991 Natural and sexual selection on many loci. *Genetics*,

137 **127**, 229–255.

Variables and Parameters Definitions

$e_{i,j,k}$

Frequency of eggs of genotype (i, j)

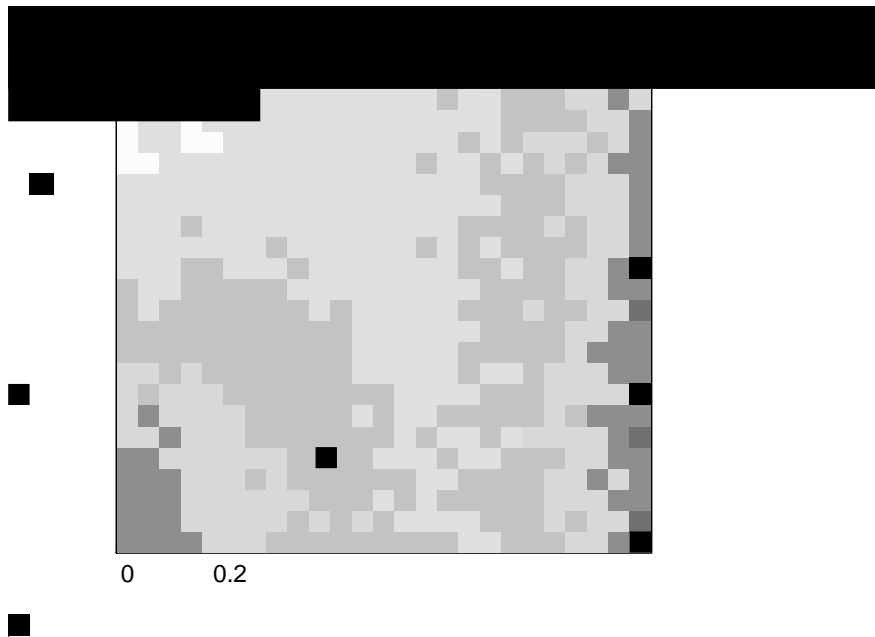
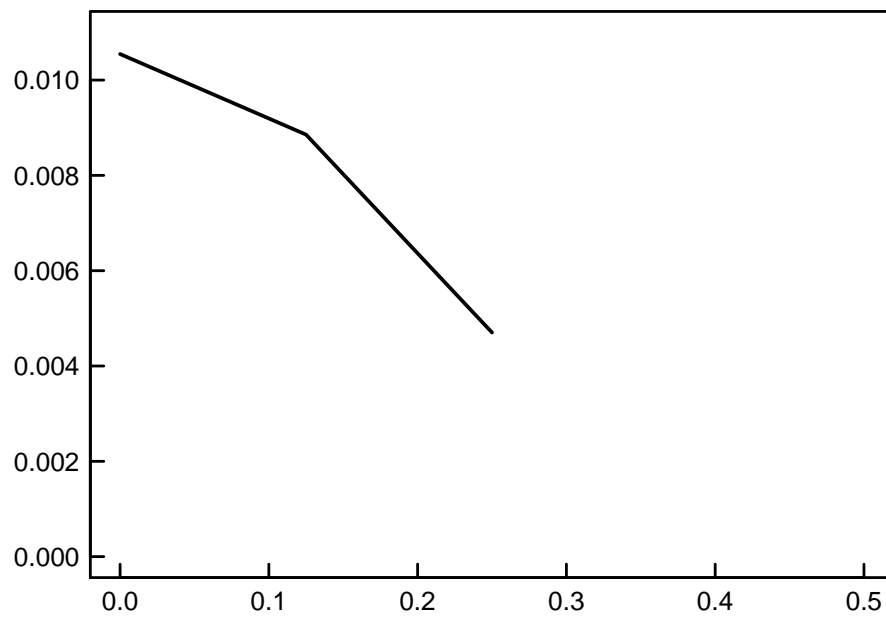


Figure S1: Evolved mutation rate in hosts after 10^7 generations as a function of the recombination rate. Each cell again represents the mean of 10 replicate simulations. To the right of the vertical black line, cycle amplitude in hosts is negligible for the duration of the evolution runs. In Fig. S2, we show vertical cross sections from this figure for $\bar{r} = 0.1$ and $\bar{r} = 0.9$ with hundred-fold replication. $v = 0.25$ and all else is as described in Fig. 3.



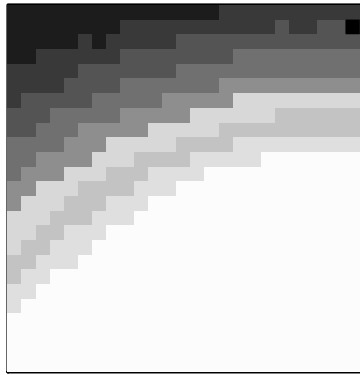


Figure S3: The critical mutation rate at which cycle size becomes negligible (amplitude < 0.1) in hosts (a) and parasites (b). All other parameters are as in Fig. 1

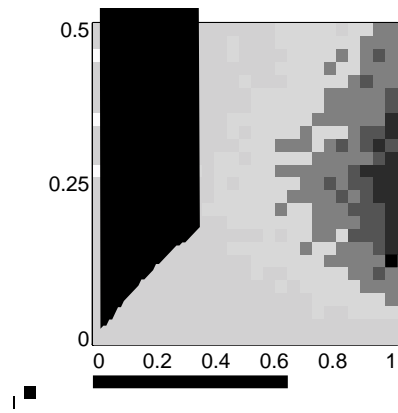


Figure S4: The difference, in hosts, between the mutation rates that evolved (i.e., those shown in Fig. 3) and the critical mutation rate at which coevolutionary cycles become negligible (amplitude < 0.1) with (a) complete linkage ($r = 0$) and (b) free recombination ($r = 0.5$). Darker shading indicates that mutation rates evolved further past the critical mutation rate and white cells indicate cases when evolved mutation rates failed to reach the critical value. The critical mutation rate at which cycle amplitude becomes negligible is shown in Fig. S3a. Previous theory has shown that mutation rates will evolve until cycles become negligible. Here we show that, with sufficiently strong maternal transmission, mutation rates will evolve past this critical value. The solid curves indicate the boundary below which cycle amplitude is negligible, even at small rates (Fig. 2).

Figure S5: Time course for the evolution of mutation rate in hosts for varying rates of maternal infection, f , and virulence, v . Parameters used for the six panels here correspond to the analogous six panels in Fig. 1. The black curve denotes the mutation rate that evolved after 10^7 generations, averaged across 10 replicate model runs, and the grey curves denote the evolved mutation rate at uniformly spaced intermediate time intervals. As can be seen here, modifier evolution has dramatically slowed by generation 10^7 , except in the case when maternal transmission is strong (panels c and f).

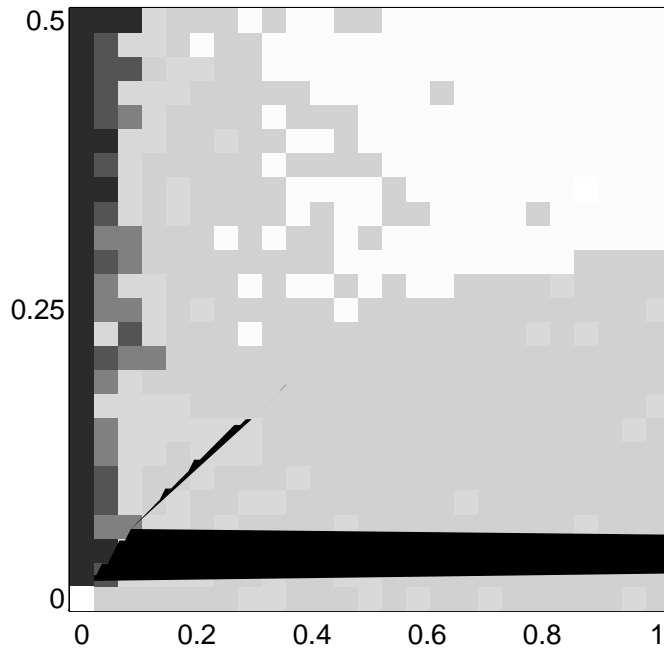


Figure S6: The difference, in parasites, between the ESS mutation rates (i.e., those shown in Fig. 5b) and the critical mutation rate at which coevolutionary cycles (measured for consistency from host dynamics) become negligible (amplitude < 0.1). Darker shading indicates that mutation rates evolved further past the critical mutation rate and white cells indicate cases when evolved mutation rates failed to reach the critical value. The critical mutation rate at which cycle amplitude becomes negligible is shown in Fig. S3b. Previous theory has shown that mutation rate in parasites will also evolve until cycles become negligible. Here we show that, with sufficiently strong maternal transmission, mutation rates in parasites will stop evolving before reaching this critical value. The solid curve indicates the boundary below which cycle amplitude in hosts is negligible, even with very small mutation rates in both species (see Fig. 2). In this region, any mutation rate evolution that occurs in parasites will, thus, lead to a positive value, even if it is occurring only by drift.